J Mater Sci (2007) 42:2758–2765
DOI 10.1007/s10853-006-1405-9

Preparation and characterization of metalorganic chemical vapor deposited nickel oxide and lithium nickel oxide thin films

M. A. Eleruja · G. O. Egharevba · O. A. Abulude · O. O. Akinwunmi · C. Jeynes · E. O. B. Ajayi

Received: 24 May 2005 / Accepted: 22 February 2006 / Published online: 12 January 2007
© Springer Science+Business Media, LLC 2007

Abstract Thin films of nickel oxide and lithium nickel oxide were deposited through the pyrolysis of nickel acetylacetonate and lithium nickel acetylacetonate, respectively in the temperature range 350–420 °C. The single solid source precursors, nickel acetylacetonate and lithium nickel acetylacetonate were prepared and characterized using Energy Dispersive X-Ray Fluorescence (EDXRF), X-Ray Diffraction (XRD) and infrared spectroscopy. The composition, optical and electrical properties of the prepared thin films were analysed using a variety of techniques, including, Rutherford Backscattering Spectroscopy (RBS), EDXRF, XRD, UV–Visible Spectrophotometry and van der Pauw conductivity method. The amount of metals in the prepared thin films did not reflect the ratio of the metals in the precursor but was found to depend on the deposition temperature. The energy gaps of the nickel oxide and lithium nickel oxide thin films are 3.7 and 3.2 eV, respectively. The electrical conductivity showed that lithium nickel oxide thin film has an activation energy of 0.11 eV. The conduction was explained by a hopping mechanism.

M. A. Eleruja · O. A. Abulude · O. O. Akinwunmi · E. O. B. Ajayi (✉)
Department of Physics, Obafemi Awolowo University, Ile-Ife, Nigeria
e-mail: eajayi@oauife.edu.ng

G. O. Egharevba
Department of Chemistry, Obafemi Awolowo University, Ile-Ife, Nigeria
e-mail: gegharev@oauife.edu.ng

C. Jeynes
University of Surrey, Ion Beam Centre, Guildford, Surrey GU2 7XH, UK
e-mail: C.Jeynes@eim.surrey.ac.uk

M. A. Eleruja
e-mail: meleruja@oauife.edu.ng

O. O. Akinwunmi
e-mail: ooakinwunmi@yahoo.com

Introduction

Transition metal oxides have generated renewed interest among research groups since the discovery of high temperature superconductors and the various interesting properties of this class of materials. More recently there has been a search for a completely inorganic electrochromic device for optical transmission modulation. Inorganic transparent electrodes in the form of transition metal oxide thin films are used as electrochromic displays (ECD's) in preference to polymers [1]. Nickel oxides, important members of this group, have been widely used for electrochromic anodes for the last decades [1]. Various deposition techniques have been used to deposit electrochromic nickel oxide and nickel-oxide-based thin films on different substrates. These include sol–gel-dip-coating technique [2], evaporation [3], RF sputtering [4], Pulsed Laser Deposition (PLD) [5] and MetalOrganic Chemical Vapour Deposition (MOCVD) [6]. A good number of properties of nickel-oxide-based thin films such as thermal [2] and structural analyses [7, 8] have been investigated.

The search for alternate energy sources has shifted attention to a sub-group of transition metal oxides, such as Mo–O [9], Li–Ni–O, Li–Co–O [10], Li–Mo–O [11], among others. The interesting properties of such materials have made them attractive for use as electrode materials in fuel cells [10, 11] and batteries for high

density [12] and high temperature batteries [13]. The metal oxides are preferred to the metal sulphides because of their reduced corrosive nature and they also have further advantage of requiring no special handling or preparation techniques since they can be prepared in air, unlike the sulphur-containing compounds [13].

NiO, a thermoelectric (TE) material, has been found to be a good material for sensing hydrogen, an attractive candidate for future energy [14], because its conductivity is easily controlled by alkali dopants [15]. This also makes lithium nickel oxide thin film a promising material for hydrogen gas sensors.

Our simple set up has been used to produce good quality thin films which have been shown to have comparable properties with those prepared via more sophisticated techniques [16, 17]. The use of single solid source metal acetylacetonates as precursors for the preparation of single and multiple metal oxide thin films has been shown to be convenient by many researchers [18, 19]. This is because it is easy to control the stoichiometry of the resulting film by modifying the composition of the precursor [18, 20] and deposition conditions.

In this paper, we report the preparation of nickel acetylacetonate and lithium nickel acetylacetonate precursors. Nickel oxide and lithium nickel oxide thin films were deposited by the pyrolysis of these single solid source precursors, nickel acetylacetonate and lithium nickel acetylacetonate, respectively. The results of the investigations of the basic properties of the deposited thin films are also presented.

Experimental methods

Preparation and characterization of nickel acetylacetonate

Nickel acetylacetonate was prepared using the method reported by Charles and Pawliskowski [21]. According to the method, 59.4 g (0.25 mol) of nickel chloride ($NiCl_2{\cdot}6H_2O$) dissolved in 250 mL of water was added to 50 mL of acetylacetone (0.5 mol) in 100 mL of methanol while stirring. The resulting mixture was added to a solution of sodium acetate (used as buffer) in 150 mL of water was heated, cooled to room temperature and placed in the refrigerator for several hours to crystallize. The green solid was filtered-off, washed and dried in a vacuum dessicator.

$$NiCl_2 \cdot 6H_2O + 2C_5H_8O_2 \rightarrow Ni(C_5H_7O_2)_2 + 2HCl + 6H_2O$$

The Infrared (IR) transmission spectrum of the nickel acetylacetonate was measured as Nujol mull (now known as the ''liquid parafin mull procedure'') at normal incidence using an IR spectrophotometer.

Preparation and characterization of lithium nickel acetylacetonate

Lithium nickel acetylacetonate was prepared using a modified form of the method reported by Ellern and Ragsdale [22]. Nickel chloride ($NiCl_2{\cdot}6H_2O$) (2.38 g) was dissolved in 27 mL of methanol and added to 1.5 g of lithium hydroxide (dissolved in methanol) and 6.2 mL of acetylacetone in 40 mL of methanol, drop-wise over a period of 2 h. The fine blue precipitate was filtered and washed with three 7–10 mL portions of methanol.

$$LiOH + NiCl_2 \cdot 6H_2O + 3C_5H_8O_2 \rightarrow Li[Ni(C_5H_7O_2)_3)] + 2HCl + 7H_2O$$

The IR transmission spectrum of the lithium nickel acetylacetonate was measured as Nujol mull (now known as the ''liquid parafin mull procedure'') at normal incidence. The elemental compositional analysis of the lithium nickel acetylacetonate was carried out using energy dispersive X-Ray fluorescence spectrometer. The X-ray diffraction pattern of the lithium nickel acetylacetonate was obtained using MD10 mini Diffractometer.

Preparation of the nickel oxide and lithium nickel oxide thin films

The thin films of nickel oxide and lithium nickel oxide were prepared using a previously reported MOCVD technique [23, 24]. Nickel oxide thin films were deposited on both stainless steel of dimensions 25×25 mm $\times$ 0.25 mm (Catalogue number FE 240300) and soda lime glass substrates, while lithium nickel oxide thin films were deposited on soda lime glass substrates. For each deposition, the precursor was ground into fine powder and poured into an unheated receptacle, from where it was blown into the heated chamber by nitrogen gas (dried over calcium chloride), at the rate of 2.5 dm^3/min (1 L/min) into the working chamber maintained at 420 °C by an electrically heated furnace for the deposition of nickel oxide thin film and 350 °C for lithium nickel oxide thin films. The soda-lime glass substrates were supported on stainless steel blocks for good and uniform thermal contact. In the hot region, the precursor first sublimed and then decomposed forming the desired

coating on the substrate. The deposition setup is shown in Fig. 1.

Characterization of nickel oxide and lithium nickel oxide thin films

The compositional analyses of the lithium nickel oxide thin films were carried out using Link analytical XRF equipment model 300 coupled to Si(Li) detector interfaced with 20 MHz multichannel analyzer system data reduction. Complementary compositional analyses of the thin films and the bare substrate were carried out using the Rutherford Backscattering Spectroscopy (RBS) using 1.5 MeV $^{4}He^{+}$. The X-ray diffraction pattern of the lithium nickel oxide thin films was obtained using MD10 mini Diffractometer for an exposure time 1200 s and radiation: Cu K_{α}. Absorbance measurements were carried out to study the optical behaviour of the thin films in the range 300–950 nm using a Unicam SP8-400 UV–visible Spectrophotometer. All measurements were made with a blank soda-lime glass substrate in the reference beam. The electrical conductivity of the lithium nickel oxide thin films was measured by the van der Pauw [25] four-probe technique over the temperature range of 303–403 K, while the carrier type was determined by the hot probe method.

Results and discussion

Infrared spectrophotometric analysis of the precursors and the thin films

Figure 2a and b show the infrared spectra obtained for nickel acetylacetonate and lithium nickel acetylacetonate in Nujol mull (now known as the ''liquid parafin mull procedure''), respectively. A close examination of the spectra shows that both systems exhibit the expected absorption frequency bands between 1700 and 1300 cm^{-1} attributable to the acetylacetonate ligand. Other absorption frequencies such as the perturbed carbonyl bands at 1616 cm^{-1} and metal–oxygen band at 700 cm^{-1} were also observed. This is in agreement with the work of Lawson [26].

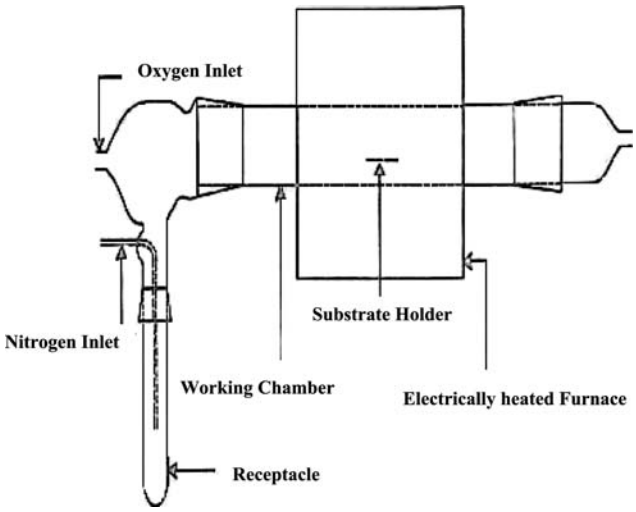

Fig. 1 Thin film deposition set-up

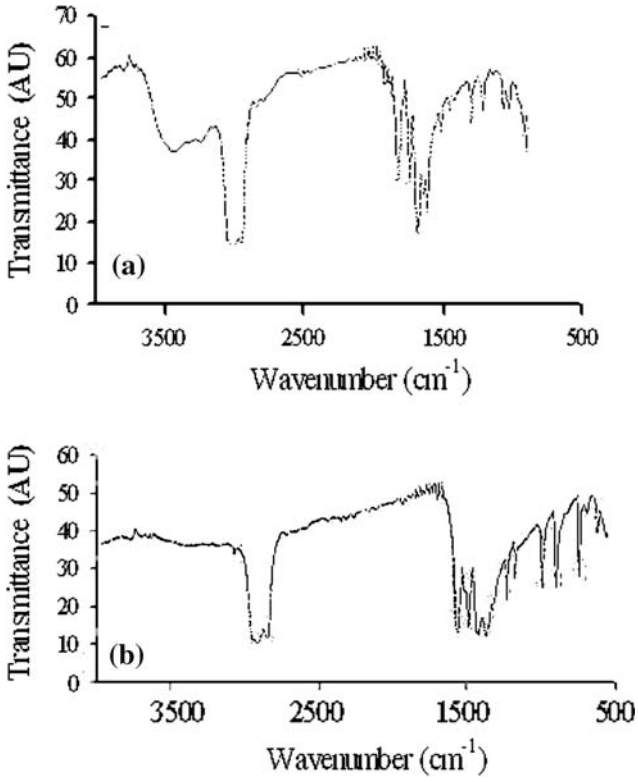

Fig. 2 (**a**) IR-spectrum of nickel acetylacetonate. (**b**) IR-spectrum of lithium nickel acetylacetonate

Compositional analysis

(a) The Energy Dispersive X-Ray Fluorescence (EDXRF) spectra of the lithium nickel acetylacetonate and the lithium nickel oxide thin films

The EDXRF spectrum for the lithium nickel acetylacetonate is presented in Fig. 3a, while that of the lithium nickel oxide thin film is presented in Fig. 3b. Three peaks are prominent in both spectra. The peak at 2.696 eV (L_{α}) is ascribed to the signal from the rhodium target of the X-ray tube in the EDXRF system while the second and third peaks at 7.477 eV (K_{α}) and 8.264 eV (K_{β}) in Fig. 3a and b are due to the presence of nickel. The areas covered by nickel in the spectra show that nickel is more abundant in the precursor than in the thin film. Lithium (Li) was not

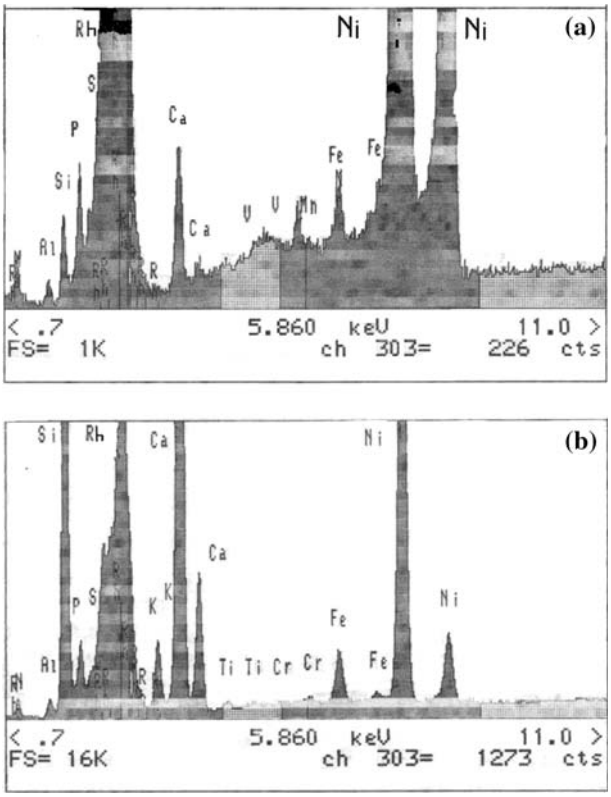

Fig. 3 (**a**) XRF spectrum of lithium nickel acetylacetonate. (**b**) XRF spectrum of lithium nickel oxide thin film

detected in both systems. This is due to the low sensitivity of EDXRF for Lithium.

(b) The RBS of nickel oxide and lithium nickel oxide thin films

The RBS spectrum of the nickel oxide thin film on stainless steel, presented in Fig. 4 was obtained for a tilted geometry (2.0 MeV $^4He^{2+}$ beam, tilted 40°). The Ni signal is at channel 369 while that of oxygen is near channel 150 where it is embedded in the signal of the stainless steel substrate.

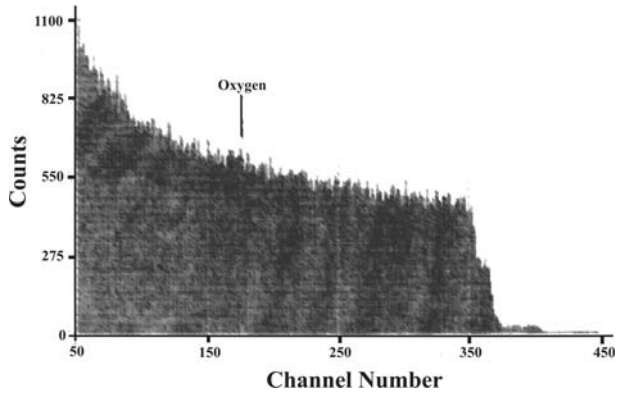

Fig. 4 RBS spectrum of nickel oxide thin film on stainless steel (2.0 MeV $^4He^{2+}$ beam, tilted 40°)

Figure 5a shows the RBS spectrum of the lithium nickel oxide thin films. There is no significant signal for lithium and the fit is not good for the O signal so there is no information on the Li:O ratio. The fit then searched for the Li:Ni:O stoichiometry, assumed constant throughout the profile, using the data furnace code [27] and found it to be 55:19:26. Bruce [28], however, reported that $LiNiO_2$ has proved impossible to prepare as a stoichiometric material. Instead compounds with the formula $Li_{1-\delta}Ni_{1+\delta}O_2$ are obtained. Figure 5b shows the depth profiling for the combined substrate and lithium nickel oxide thin film. The profile shows that there is diffusion of some of the elements across the film–substrate interface. This phenomenon has been reported earlier by Ajayi et al. [16]. The thickness of the lithium nickel oxide thin film is 182.23 nm.

X-ray diffraction study

The X-ray diffraction pattern of the lithium nickel acetylacetonate, which was collected from MD10 mini Diffractometer is shown in Fig. 6a. The intense peaks occur at diffraction angles, (2θ) = 17.7°, 18.65°, 23.53°,

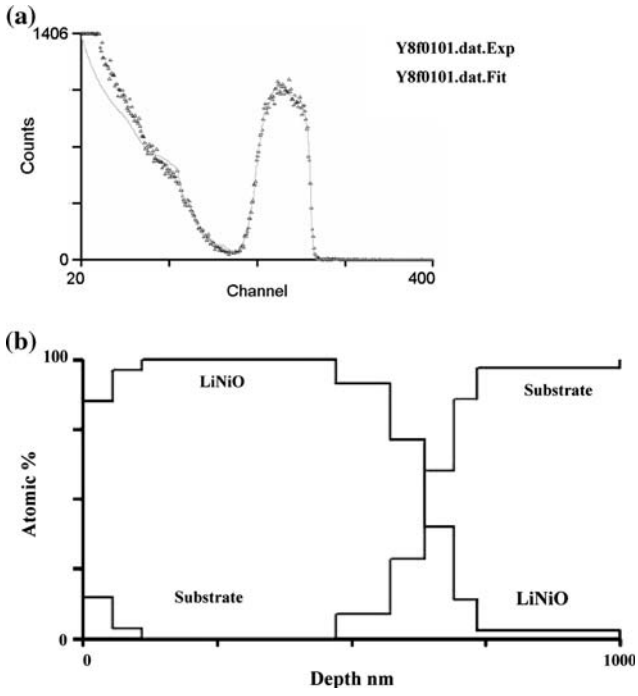

Fig. 5 (**a**) RBS Spectrum of lithium nickel oxide thin film on soda-lime glass (1.5 MeV $^4He^{2+}$ beam, detector scattering angle 147.7°). (**b**) RBS depth profiling of the combined substrate and lithium nickel oxide thin film

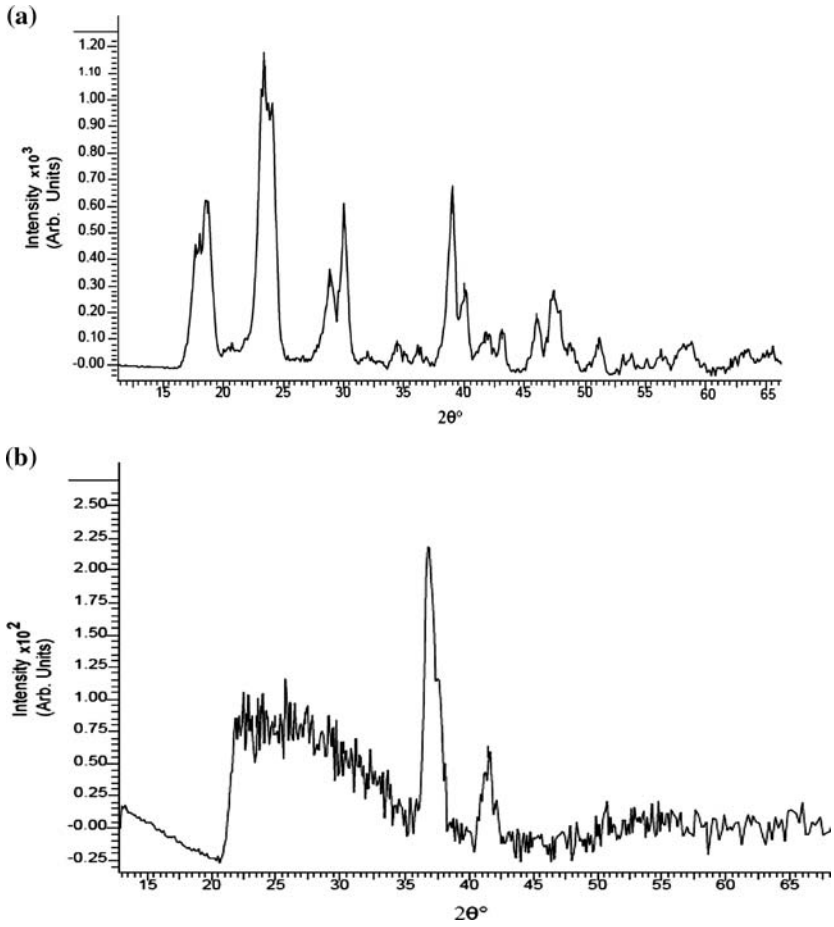

Fig. 6 (**a**) X-ray diffraction pattern of lithium nickel acetylacetonate. (**b**) X-ray diffraction pattern of lithium nickel oxide thin films

28.84° 29.99°, 38.90°, 47.43°. The intense peaks show that the precursor, lithium nickel acetylacetonate is polycrystalline in nature. The XRD peak positions and relative intensities match well with those of well-known standard of lithium acetylacetonate and nickel acetylacetonate powder materials (Card Number 33-1772, 22-1842). Figure 6b shows the XRD pattern of the lithium nickel oxide thin films. The presence of the diffraction peaks indicates that the films are polycrystalline. The strong peaks appear at diffraction angle, $(2\theta) = 25.75°$, 33.64°, 38.27°, 39.52°, 40.77°, 44.27°, 45.64°, 48.90°, 53.91°. The peak positions fitted well with the standard of lithium nickel oxide ($LiNiO_2$) (Card Number 26-1175).

While RBS could not determine the lithium oxygen ratio (Li:O) accurately, the XRD confirmed the presence of lithium, nickel and oxygen.

UV–visible spectrophotometric analysis

Figure 7a shows the absorbance spectrum of Li–Ni–O thin film while Fig. 7b shows the absorbance spectrum of the Ni–O thin film. The lithium nickel oxide thin films are highly absorbing in the ultra-violet region and more transparent in the visible region. The nickel oxide thin films are also highly absorbing in the ultra violet region and highly transmitting in the visible region. The absorption coefficient, α for both films were calculated from the relation,

$$\alpha = \frac{1}{x}\ln\frac{1}{T} \tag{1}$$

where x is the thickness of the film and $T = 10^{-A}$, T is the transmission and A is the absorbance. The absorption coefficient data were then fitted with the optical transition model [29].

$$(\alpha h\nu) = A\left(h\nu - E_g\right)^n \tag{2}$$

The analysis showed that the absorption coefficient spectra can be described by Eq. 2 with $n = 1/2$. Plots of $(\alpha h\nu)^2$ versus energy, $E(= h\nu)$ for nickel oxide and lithium nickel oxide thin films are shown in Fig. 8a and b, respectively. The relationship in each case is that

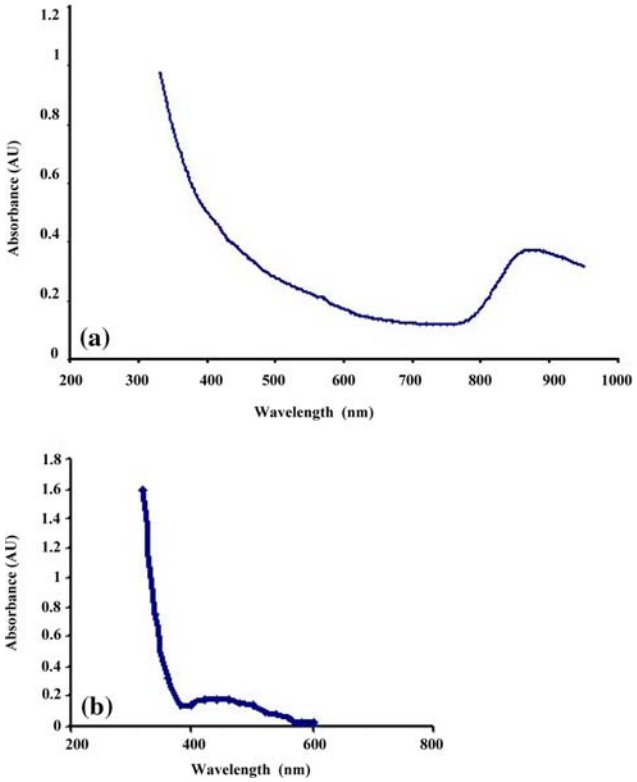

Fig. 7 (**a**) Absorbance spectrum of lithium nickel oxide thin film. (**b**) Absorbance spectrum of nickel oxide thin films

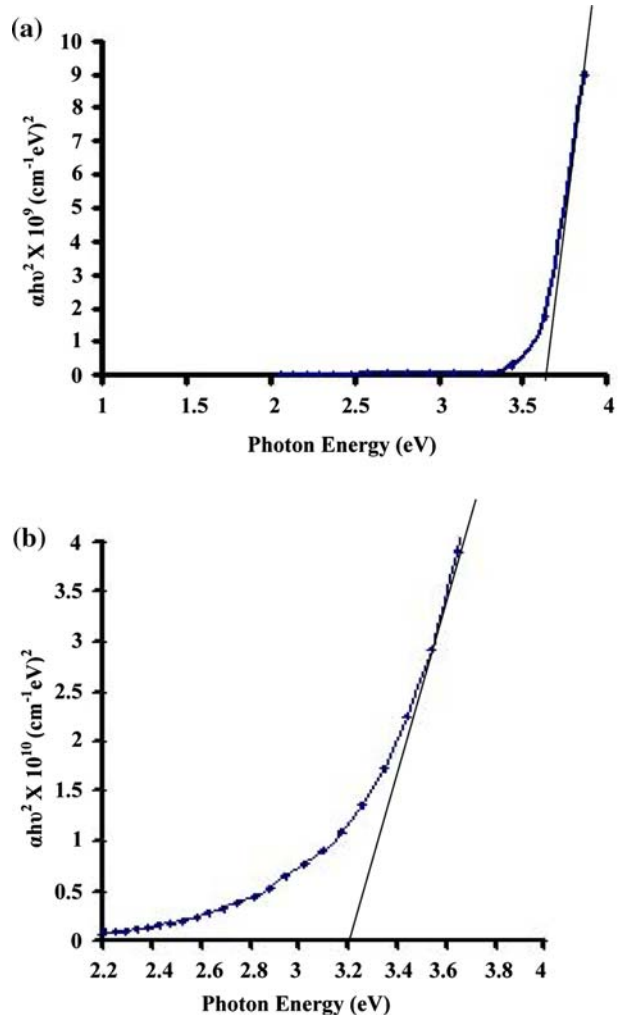

Fig. 8 (**a**) $(\alpha h\nu)^2$ versus energy for nickel oxide thin films. (**b**) $(\alpha h\nu)^2$ versus energy for lithium nickel oxide thin film

expected of a direct allowed transition. The extrapolation of the straight line regimes of the plots to $(\alpha h\nu)^2 = 0$ gave direct allowed gaps of 3.7 and 3.2 eV for the Ni–O and Li–Ni–O thin films, respectively. Wang et al. [30] have reported that NiO nanoparticles have a direct band gap of 3.56 eV, which is close to the value obtained in this work. According to Galakhov et al. [31] the doping of NiO with lithium leads to the formation of an impurity acceptor band above the O 2p valency band. This impurity band according to Kuiper et al [32] is separated by an energy gap of 0.5 eV from the top of the valency band leading to an effective energy gap of about 3.2 eV.

Electrical characterization

The electrical conductivity measurements of as deposited Li–Ni–O thin films were performed using the van der Pauw method. It was observed that the experimental data fitted well with the expression for the electrical conductivity for a semiconducting material. The results obtained can be fitted by the following equation [33]

$$\sigma_s = \frac{\sigma_0}{T^{\gamma-1}} \exp\left(\frac{-E_a}{k_B T}\right) \quad (3)$$

where $\gamma = 1$ or 2, σ_0 and E_a are constant over a substantial range of temperatures, E_a is the activation energy, σ_s is the conductivity at temperature, T. $\gamma = 1$ reduces Eq. 3 to the expression for electronic conductivity while $\gamma = 2$ reduces Eq. 3 to the expression for electrical conductivity under polaron conduction model.

In order to understand the conduction mechanism, the hopping or small polaron model was tested for by plotting a graph of $\ln \sigma T$ against the reciprocal of temperature, Fig. 9. The activation energy obtained for the hopping model is 0.11 ± 0.01 eV. Dutta et al. [34] reported that measurements of electronic transport on Li_xNiO_2 exhibit a small but definable activation energy for electronic transport associated with small polaron hopping in the mixed valence $Ni^{4+/3+}$ state.

The hopping mechanism in lithium nickel oxide can be further explained using the theories of Heikes and

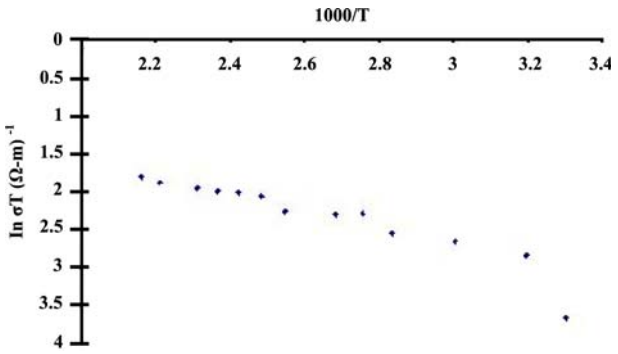

Fig. 9 ln σT versus $1/T$ for lithium nickel oxide thin film

Johnston [35] and Alder and Feinleib [36]. Heikes and Johnston [35] reported that the conduction mechanism could be considered as a thermally activated diffusion process (hopping model). They attributed the activation energy for this diffusion process to the trapping of the holes by the lattice polarization (and the accompanying lattice distortion) induced by the hole itself. This is based on the premise that the doping with lithium leads to compensation by the Ni^{3+} ion. At low temperatures the compensating holes Ni^{3+} are bound to Li^{+} ions and at high temperatures, the holes are free and move through the lattice by the interchange of electrons between Ni^{3+} and Ni^{2+} ions. However, Alder and Feinleib [36] have reported that the compensation by Ni^{3+} cannot be the correct form of charge compensation because of energetic reasons. Rather, it is assumed that the charge compensation occurs by O^{-} ions, which are also known as oxygen holes (''ligand holes''). This suggestion is strengthened by Kuiper et al. [32] when they showed using oxygen K-edge X-ray absorption spectroscopy that the holes compensating the Li^{+} impurity charge in $Li_xNi_{1-x}O$ are located in the O 2p states rather than in the conventionally assumed Ni 3d states. The explanation given by Alder and Feinleib [36] appears to be more acceptable than that of Heikes and Johnston [35] in view of the energy consideration.

Conclusion

In this work, we have prepared and characterized single solid source precursors, nickel acetylacetonate and lithium nickel acetylacetonate. We have also shown that it is possible to deposit thin films of nickel oxide (Ni–O) and lithium nickel oxide (Li–Ni–O) through the pyrolysis of the single solid source precursors. The stoichiometry of Li–Ni–O can be controlled by both the initial composition of the precursor and the temperature at which it is subsequently cracked. Our initial mixture was only chosen for convenience, but the range of solubility of the two metals in the precursor has not been investigated.

The single solid source precursors, nickel acetylacetonate and lithium nickel acetylacetonate were characterized using EDXRF, XRD and Infrared Spectrophotometry. The composition, optical and electrical properties of the prepared thin films were obtained using a variety of techniques, such as RBS, EDXRF, UV–visible spectrophotometry and the van der Pauw conductivity method. The amount of the metals in the prepared thin films did not reflect the ratio of the metals in the precursor but was found to depend on the deposition temperature. The stoichiometry of the lithium nickel oxide system was found to be $Li_{1-x}Ni_xO_{1-2x}$ (Li:Ni:O = 55:19:26) using Rutherford Backscattering Spectroscopy (RBS), under the operating conditions of the deposition chamber. XRD pattern shows that the lithium nickel oxide thin films are polycrystalline. The energy gaps of the nickel oxide and lithium nickel oxide thin films are 3.7 and 3.2 eV, respectively. The electrical conductivity showed that lithium nickel oxide thin film has activation energy of 0.11 eV. The conduction was explained by a hopping mechanism. The doping with lithium (in LiNiO) leads to charge compensation by O^{-} ions, which are also known as oxygen holes (''ligand holes''). The properties exhibited by the thin films may make them useful in various device applications.

Acknowledgement The RBS was carried out at the D. R. Chick Accelerator Laboratory, University of Surrey, so we thank the staff of the laboratory. We are grateful to the Third World Academy of Science (TWAS, Grant (93-058 R6/PHYS/AF/AC) Italy and Obafemi Awolowo University, Ile-Ife (University Research Committee (URC) for supporting this project. EDXRF was done by Femi Ogunsola of Pollution Laboratory, Obafemi Awolowo University, Ile-Ife. XRD was carried out at EMDI Laboratories, Akure, Nigeria, so we are grateful to all staff of the Institute.

References

1. Nagai J, Morisaki S (2003) Solid State Ionics 165:149
2. Cere Korosec R, Bukovec P (2004) Thermochim Acta 410:65
3. Stanescu S, Boeglin C, Barbier A, Deville J-P (2004) Surf Sci 549:172
4. Urbano A, de Castro SC, Landers R, Morais J, Sieervo AD, Gorenstein A, Tabacniks MH, Fantini MCA (2001) J Power Sources 97(98):328
5. Wen S-J, von Rottkay K, Rubin M (1997) Proc Electrochem Soc PV 96(24):54
6. Eleruja MA (1998) Ph.D Thesis, Obafemi Awolowo University, Ile-Ife, Nigeria, (Unpublished)

7. Sakata O, Yi MS, Matsuda A, Liu J, Sato S, Akiba S, Sasaki A, Yoshimoto M (2003) Appl Surf Sci 221:450
8. Avendano E, Azens A, Isidorsson J, Karmhag R, Niklasson GA, Granquist CG (2003) Solid State Ionics 165:169
9. Ilori OO, Osasona O, Eleruja MA, Egharevba GO, Adegboyega GA, Chiodelli G, Boudreault G, Jeynes C, Ajayi EOB (2005) Thin Solid Films 472:84
10. Kwon CW, Hwang SJ, Delville MH, Labrugere C, Murugan AV, Kale, Vijayamohanan K, Campet G (2003) Active Passive Electron Components 26:23
11. Choy JH, Kim DH, Kwon CW, Hwang SJ, Kim YI (1999) J Power Sources 77:4316
12. Mizushuma K, Jones PC, Wiseman PJ, Goodenough JB (1980) Mat Res Bull 15:783
13. Godshell NA, Raistrick ID, Huggins RA (1980) Mat Res Bull 15:561
14. Shin W, Imai K, Izu N, Murayama N (2001) Jpn J Appl Phys 40:L1232
15. Shin W, Murayama N (2000) Mater Lett 45:302
16. Ajayi OB, Akanni MS, Lambi JN, Jeynes C, Watts JF (1990) Thin Solid Films 185:123
17. Adedeji AV, Egharevba GO, Jeynes C, Ajayi EOB (2002) Thin Solid Films 402:49
18. Bott S, Fahlman BD, Pierson ML, Barron AR (2001) J Chem Soc Dalton Trans 2148
19. Behrsing T, Bond AM, Deacon GB, Forsyth CM, Forsyth M, Kamble KJ, Skelton BW, White AH (2003) Inorg Chim Acta 352:229
20. Akinwunmi OO, Eleruja MA, Olowolafe JO, Adegboyega GA, Ajayi EOB (1999) Opt Mat 13:255
21. Charles RG, Pawliskowski MA (1958) J Phys Chem 62:440
22. Ellern JB, Ragsdale RO (1968) Inorg Syn 11:87
23. Ajayi OB (1970) M.Sc. Thesis, University of Illinois, Urbana Illinois
24. Ajayi OB, AnaniAA, Obabueki AO (1981) Thin Solid Films 82:151
25. van der Pauw LJ (1958) Philips Rep 15:1
26. Lawson KE (1961) Spectrochim Acta 17:248
27. Jeynes C, Barradas NP, Marriott PK, Boudreault G, Jenkin M, Wendler E, Webb RP (2003) J Phys D 36:R97
28. Bruce PG (1997) Chem Commun 1817
29. Bube RH (1974) Electronic properties of crystalline solids. Academic Press, London, p 417
30. Wang X, Song J, Gao L, Jin J, Zheng H, Zhang Z (2005) Nanotechnology 16:37
31. Galakhov R, Kurmaev EZ, Uhlenbrock St, Neumann M, Kellerman DG, Gorshkov VS (1995) Solid State Commun 95:347
32. Kuiper P, Kruiziriga K, Ghijsen J, Sawatzky GA, Verweij H (1989) Phys Rev Lett 62:221
33. Ali-Omar M (1975) Elementary solid state physics. Addison-Wesley, Reading, MA, p 275
34. Dutta G, Manthiram A, Goodenough JB, Grenier J-C (1992) J Solid State Chem 96:123
35. Heikes RR, Johnston WD (1957) J Chem Phys 26:582
36. Adler D, Feinleib J (1970) Phys Rev B 2:3112